Computational Study of the Reaction between Biogenic Stabilized Criegee Intermediates and Sulfuric Acid

Theo Kurtén,* Boris Bonn, Hanna Vehkamäki, and Markku Kulmala

Department of Physical Sciences, University of Helsinki, P. O. Box 64, FIN-00014 Helsinki, Finland

Received: November 24, 2006; In Final Form: February 21, 2007

We have postulated a mechanism for the reaction of sulfuric acid with stabilized Criegee intermediates (sCIs). We have computed Gibbs free energies for the reaction of sulfuric acid with two biogenic sCIs and three smaller model species. We have also calculated Gibbs free energies for two competing sink reactions. Due to the large size of the biogenic sCIs, the computations have been performed at the relatively modest B3LYP/6-31G(d,p) and B3LYP/6-311+G(2d,p) levels. However, single-point RI-CC2/def2-QZVPP calculations for the $(CH_3)_2COO$ model species are in good agreement with the B3LYP results. The reaction is found to be strongly exothermic for all studied species. Activation barrier calculations on the $(CH_3)_2COO$ model species further indicate that the reaction with sulfuric acid may proceed significantly faster than the sink reaction with water. If the same applies to the biogenic sCIs, the proposed reactions could account for some part of the organically assisted new particle formation events observed in the atmosphere.

Introduction

Aerosol particles play an important role in the climate system,[1] and have a significant influence on human health.[2] The formation of aerosol particles via gas-to-particle nucleation is one of the least-understood aerosol-related processes, and one of the major sources of uncertainty, e.g., in climate models. In the troposphere, new particle formation is thought to involve sulfuric acid and water molecules, with possible contributions from ions, ammonia, or some organic species.[3−7] However, the identity of the participating organic species is so far unknown. A recent study by Zhang et al.[8] explained nucleation in the presence of sulfuric acid during aromatic volatile organic carbon oxidation by the formation of aromatic acid−sulfuric acid complexes. These complexes would have a reduced nucleation barrier due to their large size. While aromatic compounds may be important for nucleation in polluted conditions, biogenic secondary aerosol formation is likely to involve reaction products of various alkene species, such as mono- and sesquiterpenes.[9]

Previous experimental studies on particle formation during alkene oxidation have tried to explain nucleation with different compounds and processes. For example, Winterhalter et al.[10] suggested that detected dicarboxylic acids are the compounds of lowest volatility, and thus responsible for the start of nucleation. Kückelmann et al.[11] assumed that nucleation in pinene ozonolysis is started by the formation of a dimer from a pinic and a pinonic acid molecule. However, in a simulation study on secondary organic aerosol formation from α-pinene, Kamens et al.[12] could not achieve a high particle formation rate by assuming homogeneous nucleation of any of the suggested compounds, and there was a large delay before the onset of nucleation. By contrast, they found agreement with experimental results concerning the onset of nucleation after assuming the formation of a tiny core, which allowed the partitioning of further compounds on it. This core needed to be sufficiently large, so they used the largest compound they knew to exist in the system, i.e., a secondary ozonide formed from the bimolecular reaction of a so-called stabilized Criegee intermediate with pinonaldehyde.

Shortly afterward, the involvement of stabilized Criegee intermediates in particle formation was supported by experimental studies of Bonn et al.[13−15] They found that particle number concentrations decreased when water vapor was added to the reacting system. The more water vapor or formic acid was added, the later the onset of nucleation occurred, and the lower the particle formation rate that was observed. By contrast, the addition of carbonyl compounds, especially larger aldehydes, enhanced nucleation rates, and shortened the time before the onset of nucleation was observed. This can be explained by the reactions of the stabilized Criegee intermediates.

Formation and Reactions of Stabilized Criegee Intermediates

Stabilized Criegee intermediates (sCIs), first proposed by Rudolph Criegee[16] in a study of liquid-phase olefin ozonolysis, are C−O−O biradicals formed in the ozonolysis of alkenes. Criegee proposed that ozone first adds to the carbon−carbon double bond, forming a primary ozonide with high excess energy. This excess energy causes the ozonide to decompose instantaneously to the Criegee biradical, which still possesses excess energy in the form of vibrational excitations. There are three possible fates for the biradical: (a) it restructures and splits off an OH radical, forming an unsaturated hydroperoxide (hydroperoxide channel), (b) it forms an ester (ester channel, usually of minor importance), or (c) it is collisionally stabilized and becomes the stabilized Criegee intermediate. The reaction schematic is presented in Figure 1. The stabilized Criegee radical can then react with, e.g., water, aldehydes, or organic acids, forming a hydroxy-hydroperoxide, secondary ozonide (SOZ), or alkylhydroperoxycarboxylate, respectively. For large biogenic sCIs, where the original double bond split in the ozonolysis was located in a cyclic structure, SOZ formation may occur unimolecularly, with the carbonyl group formed in the ozonolysis reaction reacting with the COO group. The relative yields

* Corresponding author. E-mail: theo.kurten@helsinki.fi.

10.1021/jp067817k CCC: $37.00
Published on Web 04/10/2007

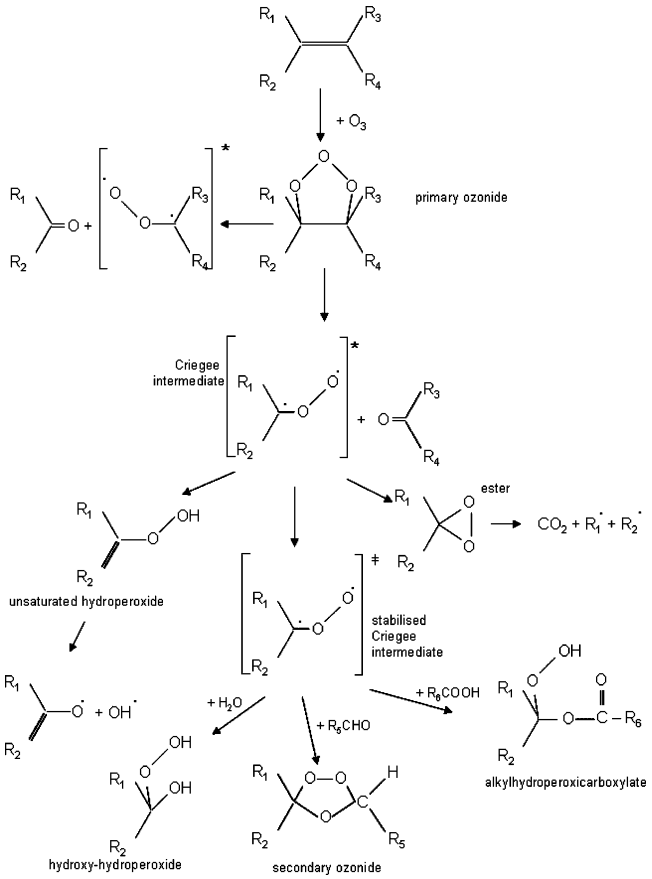

Figure 1. Reaction schematic showing formation and sink reactions of stabilized Criegee intermediates (sCIs). R_1-R_6 are functional groups.

of the different channels depends strongly on the structure of the alkene. Stabilization becomes more and more important with the size of the parent alkene. For example, Chuong et al.[17] have computationally investigated endocyclic alkene ozonolysis for different carbon numbers. They predicted that the transformation from a chemically activated to a collisionally stabilized behavior is to be expected between mono- and sesquiterpenes.

A further indication for the influence of sCI on secondary organic aerosol formation is given by a study of Tolocka et al.[18] They show that both hydroperoxide and stabilization channels are active in aerosol (mass) production. Recent, unpublished box model simulations[19] of α-pinene−ozone reactions, including aerosol dynamics, were found to reproduce aerosol size distributions and number concentrations observed in smog chambers when nucleation was assumed to start by the reaction of sCIs with carbonyl compounds (forming secondary ozonides).

Recent (unpublished) studies[20] on atmospheric nucleation events and their origin indicates that the findings in smog chambers can be used to explain new particle formation events in the boreal forest environment. However, nucleation rates have been observed to depend strongly on sulfuric acid concentrations, and predicted secondary ozonide sources are too small to explain nucleation by the reactions of organic compounds alone. Thus, another nucleation mechanism, probably not present in smog chambers, needs to be included. One such mechanism is the reaction of sCIs with sulfuric acid yielding an organic sulfate. This reaction, analogous to the sulfuric acid + aromatics mechanism presented by Zhang et al.,[8] might potentially be very significant in explaining observed nucleation events. However, nothing is known about the thermodynamics or kinetics of this reaction.

There are few studies on the absolute reaction rates of sCIs. Relative rates for reactions of sCIs with various compounds have been measured[13,21−25] by the addition of different compounds competing for the reaction. An overview on the relative rates can be found in Table 1. The greater reaction rate of formic acid with sCIs explains nicely the stronger depressing effect of the acid on nucleation compared to that of water. It can be seen from Table 1 that the sCIs generally react faster with acids than with water, and that the difference in rate constants is greater for larger sCIs than for smaller ones. Since sulfuric acid is a much stronger acid than formic acid, it is plausible that the relative rate constant for the sCI + H_2SO_4 reaction might be greater still. The purpose of this article is to investigate computationally the reaction of various sCIs with sulfuric acid, and to compare the obtained reaction parameters with those of the competing sink reactions. Due to the difficulty of finding and optimizing transition states for reactions with low barriers, we have computed activation barriers only for the reactions of the model species dimethyl carbonyl oxide. For the reactions of the larger biogenic sCIs, only thermodynamic parameters (reaction energies) are computed.

A large number of computational studies on the formation, decomposition, and reactions of various Criegee intermediates have been published.[17,26−37] However, most of them have focused on the reactions of small (one to four carbon atoms) sCIs, and have investigated primarily unimolecular decomposition pathways instead of bimolecular reactions. To our knowledge, there exists no previous study on the reaction of any sCI with sulfuric acid.

TABLE 1: Relative Experimentally Measured Rates (compared to the Reaction with Water) of Various sCIs with Different Reactants

reaction	relative rate (k_{sCI+X}/k_{sCI+H_2O})	reference
$CH_2OO + CO$	8	Su et al.[21]
$CH_2OO + O_3$	11	Su et al.[21]
$CH_2OO + NO_2$	61	Hatakeyama et al.[22]
$CH_2OO + SO_2$	170	Hatakeyama et al.[22]
$CH_2OO + NO$	610	Hatakeyama et al.[22]
$CH_2OO + HCHO$	700	Neeb et al.[23]
$CH_2OO + HCOOH$	1400	Neeb et al.[24]
$CH_3(CH_2)_{11}CHOO + CH_3OH$	22	Tobias and Ziemann[25]
$CH_3(CH_2)_{11}CHOO + CH_3CH(OH)CH_3$	50	Tobias and Ziemann[25]
$CH_3(CH_2)_{11}CHOO + HCHO$	2700	Tobias and Ziemann[25]
$CH_3(CH_2)_{11}CHOO + HCOOH$	6700	Tobias and Ziemann[25]
$CH_3(CH_2)_{11}CHOO + CH_3(CH_2)_5COOH$	17000	Tobias and Ziemann[25]
β-pinene C_9-sCI + HCHO	1000	Bonn[13]
β-pinene C_9-sCI + HCOOH	17000	Bonn[13]

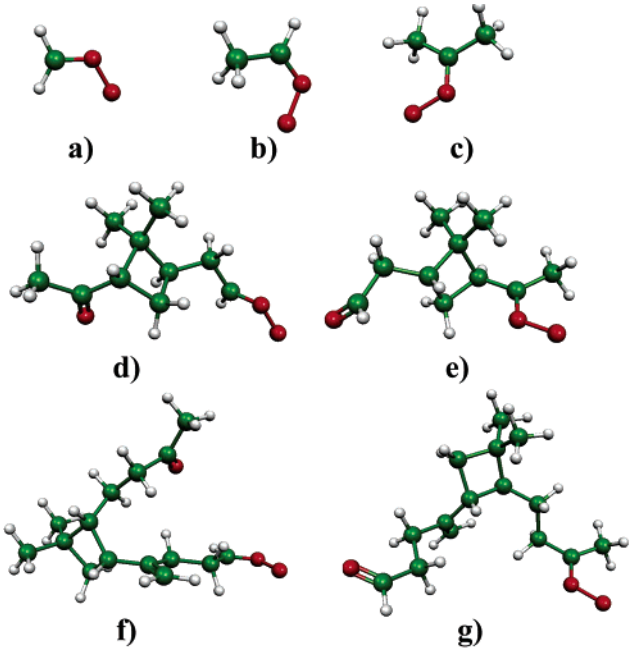

Figure 2. Structures of the Criegee intermediates studied in this work, optimized at the B3LYP/6-311+G(2d,p) level. White = hydrogen, green = carbon, and red = oxygen atoms. (a) H_2COO, (b) CH_3HCOO, (c) $(CH_3)_2COO$, (d) primary α-pinene-sCI, (e) secondary α-pinene-sCI, (f) primary *β*-caryophyllene-sCI, and (g) secondary *β*-caryophyllene-sCI.

Computational Details

Our density functional theory (DFT) calculations have been performed using the Gaussian 03 program suite.[38] The coupled-cluster single-point calculations were performed using the Turbomole program[39,40] (version 5.8). All the geometries were converged to a root mean square (RMS) and maximum force of less than 3×10^{-4} and 4.5×10^{-4} au, respectively. The convergence with respect to the electronic energy in the self-consistent field (SCF) step was 1×10^{-6} au. For the DFT calculations, the standard integration grid was used. The methods we used were the B3LYP hybrid functional[41,42] and the coupled-cluster method RI-CC2.[43,44] The basis sets included were the 6-31G(d,p) and def2-QZVPP[45] Gaussian basis sets, and a slightly modified version of the 6-311+G(2d,p) basis set with diffuse and extra p-type polarization functions added to the water and sulfuric acid hydrogen atoms in order to better describe possible hydrogen bonding within the reaction products. This modified basis set is henceforth denoted as 6-311+G(2d,p)′. (Note that for species which do not contain water or sulfuric acid the modified and original 6-311+G(2d,p) basis sets are identical.) The auxiliary basis set used in the RI-CC2/def-QZVPP calculations is described in ref 46. Gibbs free energies have been computed using the standard rigid rotor and harmonic oscillator approximations.

The biradical nature of the sCIs makes accurate quantum chemical predictions of reaction energetics or kinetics difficult, as most common computational methods do not account for multireference effects. However, Cremer et al.[27] demonstrated that relatively modest B3LYP/6-31G(d,p) and B3LYP/6-311+G(3df,3pd) calculations reproduce the multireference MR-AQCC/6-311+G(3df,3pd) results reasonably well when applied to the formation and decomposition reactions of the H_2COO, CH_3HCOO, and $(CH_3)_2COO$ sCIs. Similar results were reported by Pérez-Casany et al.,[47] who studied the reaction of the NO_3 radical with propene, and found that the deviation of B3LYP/6-31G* geometries from CASSCF(5,6)/6-31G* ones were reasonably small. Furthermore, they found a better agreement with experiments for some B3LYP activation barriers compared to CASSCF ones, with the errors of the latter method being attributed to the difficulties in "defining an active space coherent along all the potential energy hypersurface".

Test calculations were carried out to determine whether the spin-unrestricted form of the B3LYP functional would describe the electronic structure of the sCIs better than the normal restricted form. (Some studies[48] have indicated that using spin-unrestricted DFT can increase the reliability of calculations on systems with biradical nature.) However, for all tested cases (including the H_2COO, $(CH_3)_2COO$, and α-pinene-derived sCIs, along with the transition states described later) the UB3LYP and B3LYP energies and vibrational wavenumbers were identical, even when the symmetry of the initial guess wave function was broken with the Guess=Mix keyword. Furthermore, stability tests using the Stable=Opt keyword found no evidence of wave function instabilities. These tests in no way contradict the well-established result that the sCIs have a partial biradical nature; they simply indicate that switching to spin-unrestricted B3LYP does not change the results, and is thus not worth the added computational effort. Therefore, all the following calculations were carried out using the standard spin-restricted form of the B3LYP functional.

Results and Discussion

We have studied the reactions of five different organic molecules: the model species H_2COO (methyl carbonyl oxide), CH_3HCOO (ethyl carbonyl oxide), $(CH_3)_2COO$ (acetone carbonyl oxide or dimethyl carbonyl oxide), and the stabilized Criegee intermediates formed in the ozonolysis of α-pinene and *β*-caryophyllene (henceforth referred to as α-pinene-sCI and *β*-caryophyllene-sCI, respectively). For the CH_3HCOO sCI, we have chosen the "syn" isomer as it is predicted[34] to be more stable than the "anti" configuration. For the α-pinene and *β*-caryophyllene derivatives, there are two structurally different sCI isomers, as the two carbon atoms participating in the double bond split during ozonolysis are not identical. We have denoted the two structural isomers "primary" and "secondary" depending on the degree of substitution of the COO group. The optimized structures of the H_2COO, CH_3HCOO, and $(CH_3)_2COO$ model species and the four different biogenic isomers are shown in Figure 2. (All molecular structures have been drawn using the MOLEKEL program.[49]) The corresponding electronic and free energies for the biogenic isomers at the B3LYP/6-311+G(2d,p) level are shown in Table 2. (The full thermodynamic data for all studied structures are given in the Supporting Information.) Table 2 shows that, for the biogenic sCIs, the secondary isomers

TABLE 2: Electronic Energies and Gibbs Free Energies at 298 K of the Studied Biogenic Stabilized Criegee Intermediate Species, at the B3LYP/6-311+G(2d,p) Level

species	E_0, hartree	G(298 K), hartree
primary α-pinene-sCI ($C_{10}H_{16}O_3$)	−616.387 97	−616.186 74
secondary α-pinene-sCI ($C_{10}H_{16}O_3$)	−616.392 89	−616.191 31
primary *β*-caryophyllene-sCI ($C_{15}H_{24}O_3$)	−811.779 81	−811.469 19
secondary *β*-caryophyllene-sCI ($C_{15}H_{24}O_3$)	−811.788 20	−811.479 22

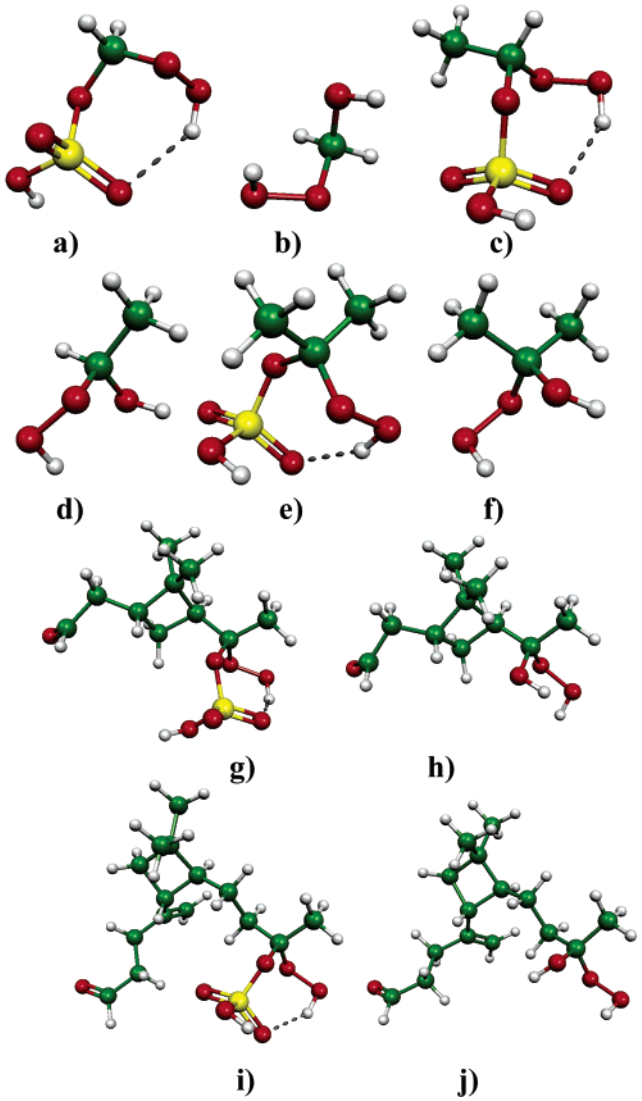

Figure 3. Structures of the sCI + H_2O and sCI + H_2SO_4 reaction products studied in this work, optimized at the B3LYP/6-311+G(2d,p) level, with diffuse basis functions and an additional set of p-type polarization functions on the H_2O and H_2SO_4 hydrogen atoms. Sulfur atoms are shown in yellow. (a) $H_2C(OOH)-O-SO_3H$, (b) $H_2C(OOH)-OH$, (c) $CH_3HC(OOH)-O-SO_3H$, (d) $CH_3HC(OOH)-O-H$, (e) $(CH_3)_2C(OOH)-O-SO_3H$, (f) $(CH_3)_2C(OOH)-OH$, (g) $C_{10}H_{18}O_7S$, (h) $C_{10}H_{18}O_4$, (i) $C_{15}H_{26}O_7S$, and (j) $C_{15}H_{26}O_4$.

(in which the COO group is stabilized by alkyl groups on both sides) are more stable than the primary ones by several kilocalories per mole. All following calculations have thus been carried out on the secondary isomers only.

We have postulated that the first reaction steps of sCIs with H_2SO_4 proceed similarly to the corresponding reaction with water.[26,36] After the initial formation of a hydrogen-bonded complex, one of the H_2SO_4 protons is transferred to the COO group, while a new bond is formed between one of the acid oxygens and the COO carbon. The $R_1R_2C(OOH)-O-SO_3H$ peroxysulfate complexes thus formed are likely to react further, but the C−O−S bonds should be quite strong and are unlikely to be broken very quickly. Thus, all subsequent products should still have high molecular masses, and probably participate efficiently in particle formation.

The products of the sCI + H_2O and sCI + H_2SO_4 reactions for all five studied sCI species are shown in Figure 3. The corresponding reaction energies and Gibbs free energies are given in Table 3. For the biogenic sCIs, unimolecular secondary ozonide (SOZ) formation is another possible sink reaction, which in atmospheric conditions competes with the bimolecular reactions. The optimized structures of the secondary ozonides formed from the α-pinene-sCI and *β*-caryophyllene-sCI species are shown in Figure 4. The corresponding reaction energies and Gibbs free energies are given in Table 4. All reaction energies were calculated with the B3LYP density functional. To assess the effect of basis set size on the energetics, two basis sets have been used: the small 6-31G(d,p) set and the medium-size 6-311+G(2d,p)′ set. (See Computational Details for the definition of the 6-311+G(2d,p)′ basis set.) The reaction energies calculated with the smaller 6-31G(d,p) basis set are consistently more negative than those calculated with the 6-311+G(2d,p)′ set. This is almost certainly due to basis set superposition error. This probably even applies to the unimolecular SOZ formation reaction, as the product SOZ is more compact than the reactant sCI, allowing a larger degree of superposition. However, the differences between the energetics of the various studied reactions are not very strongly affected by the basis set.

It can be seen from Table 3 that the bimolecular reactions with water and sulfuric acid are strongly exothermic for all studied species. The values for the $H_2COO + H_2O$ reaction agree with those presented by Aplincourt and Ruiz-Lopez[26] at the B3LYP/6-31G(d,p) level. The ΔG value of −22.2 kcal/mol for the $(CH_3)HCOO + H_2O$ reaction computed using the larger basis set is also in reasonable agreement with the value of −25.4 kcal/mol computed by Anglada et al.[36] at the CCSD(T)/6-311+G(2d,2p) level, with geometries optimized at the B3LYP/6-311+G(2d,2p) level and vibrational contributions computed at the B3LYP/6-31G(d,p) level. However, our larger basis ΔG value for the $(CH_3)_2COO + H_2O$ reaction is −16.44 kcal/mol, while that reported by Anglada et al. is −23.1 kcal/mol. A comparison of the ΔE_0 values of Anglada et al. (given in the supporting information of their article) shows that the main reason for the disagreement is the CCSD(T)6-311+G(2d,2p) − B3LYP/6-311+G(2d,2p) energy difference: for the $(CH_3)_2$-$COO + H_2O$ reaction it is −7.7 kcal/mol, while it is only −4.7 kcal/mol for the $(CH_3)HCOO + H_2O$ reaction. (The possible reasons for the quite large CCSD(T) − B3LYP differences are beyond the scope of this study.) The remaining differences between our results and those of Anglada et al. are probably related to the presence of diffuse functions on the H_2O hydrogen atoms in our study, or the use of vibrational scaling factors in theirs. It should be noted that the ΔG value of Anglada et al. is quite close to our B3LYP/6-31G(d,p) value of −24.64 kcal/mol, and that our two values bracket theirs.

For the three model species, the exothermicity decreases as the number of methyl side groups grows. This is probably due to an increasing stabilization of the biradical C−O−O group of the reactant sCI, as described, e.g., by Cremer et al.[27] and Fenske et al.[31] A similar phenomenon probably explains the relatively large differences observed between the reaction energies for the reactions of the *β*-caryophyllene- and α-pinene-derived sCIs with sulfuric acid. In the *β*-caryophyllene-sCI, the C−O−O group is located close to the end of a long unbranched carbon chain. In contrast, the α-pinene-sCI C−O−O group is adjacent to a four-carbon ring, which is presumably better able to stabilize it. Thus, it is not surprising that the energetics for the *β*-caryophyllene-sCI reactions are closer to those of the $(CH_3)_2COO$ model species than to those of the α-pinene-sCI.

SOZ formation is moderately exothermic for both studied species, in agreement with the results of Chuong et al.,[17] who reported a reaction energy of −28.8 kcal/mol at the B3LYP/6-31G(d) level for the SOZ formation of the sCI formed in the

TABLE 3: Reaction Energies and Gibbs Free Energies at 298 K for the Reactions of Various Stabilized Criegee Intermediates with Sulfuric Acid and Water[a]

reaction	ΔE_0, kcal/mol	ΔG(298 K), kcal/mol
$H_2COO + H_2SO_4 \Rightarrow H_2C(OOH)-O-SO_3H$	−42.02[b]	−27.20[b]
	−49.06[c]	−33.74[c]
$H_2COO + H_2O \Rightarrow H_2C(OOH)-OH$	−43.57[b]	−29.38[b]
	−50.69[c]	−36.23[c]
$(CH_3)HCOO + H_2SO_4 \Rightarrow (CH_3)HC(OOH)-O-SO_3H$	−34.93[b]	−19.53[b]
	−42.63[c]	−26.96[c]
$(CH_3)HCOO + H_2O \Rightarrow (CH_3)HC(OOH)-OH$	−36.40[b]	−22.20[b]
	−44.25[c]	−29.64[c]
$(CH_3)_2COO + H_2SO_4 \Rightarrow (CH_3)_2C(OOH)-O-SO_3H$	−29.95[b]	−13.97[b]
	−38.65[c]	−22.02[c]
$(CH_3)_2COO + H_2O \Rightarrow (CH_3)_2C(OOH)-OH$	−30.77[b]	−16.44[b]
	−39.41[c]	−24.64[c]
$C_{10}H_{16}O_3 + H_2SO_4 \Rightarrow C_{10}H_{18}O_7S$ (184.11 amu, 282.08 amu)	−23.37[b]	−7.90[b]
	−31.94[c]	−15.93[c]
$C_{10}H_{16}O_3 + H_2O \Rightarrow C_{10}H_{18}O_4$ (184.11 amu, 202.12 amu)	−27.36[b]	−12.75[b]
	−36.54[c]	−21.42[c]
$C_{15}H_{24}O_3 + H_2SO_4 \Rightarrow C_{15}H_{26}O_7S$ (252.17 amu, 350.14 amu)	−30.02[b]	−13.68[b]
	−38.94[c]	−22.18[c]
$C_{15}H_{24}O_3 + H_2O \Rightarrow C_{15}H_{26}O_4$ (252.17 amu, 270.18 amu)	−29.23[b]	−14.69[b]
	−38.49[c]	−23.22[c]

[a] For simplicity, only stoichiometric formulas are presented for the mono- and sesquiterpene-derived species. ($C_{10}H_{16}O_3$ corresponds to the α-pinene-sCI and $C_{15}H_{24}O_3$ to the β-caryophyllene-sCI.) For reference, the atomic masses of the reactant and product biogenic molecules are also given. [b] At the B3LYP/6-311+G(2d,p) level, with diffuse functions and extra p-type polarization functions on the H_2SO_4 and H_2O hydrogen atoms. [c] At the B3LYP/6-31G(d,p) level.

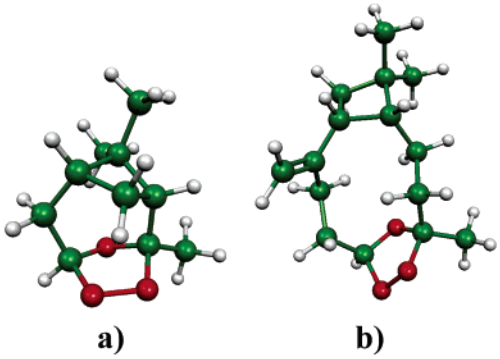

Figure 4. Structures of the secondary ozonides formed from the unimolecular reactions of the sCIs derived from (a) α-pinene and (b) β-caryophyllene, optimized at the B3LYP/6-311+G(2d,p) level.

TABLE 4: Reaction Energies and Gibbs Free Energies at 298 K for the Formation of Secondary Ozonides

reaction	ΔE_0, kcal/mol	ΔG(298 K), kcal/mol
α-pinene-sCI ⇒ α-pinene-SOZ	−19.11[a]	−11.49[a]
	−28.10[b]	−20.16[b]
β-caryophyllene-sCI ⇒ β-caryophyllene-SOZ	−17.43[a]	−6.96[a]
	−26.76[b]	−16.17[b]

[a] At the B3LYP/6-311+G(2d,p) level. [b] At the B3LYP/6-31G(d,p) level.

ozonolysis of cyclohexene. This is very close to the value of −28.1 kcal/mol computed here for the SOZ formation of the α-pinene-derived sCI at the B3LYP/6-31G(d,p) level.

Activation Barriers. As almost all the reactions studied here are exothermic, thermodynamics alone cannot yield information on the atmospheric significance of the sCI + H_2SO_4 reaction. We have therefore attempted to obtain order-of-magnitude information on the relative rates of the two bimolecular reactions by optimizing their transition states and calculating the corresponding activation barriers. Due to the high computational demand of kinetics calculations, we have studied only the $(CH_3)_2COO$ model species. Unfortunately, the small size of the molecule (and lack of a second carbonyl group) means that we are unable to estimate activation barriers for the competing unimolecular SOZ formation reaction. Chuong et al.[17] reported a barrier of 5.1 kcal/mol at the B3LYP/6-31G(d) level for the SOZ formation of the sCI formed in cyclohexene ozonolysis, with a corresponding sCI lifetime of about 70 ns. Based on the comparison of our 6-31G(d,p) and 6-311+G(2d,p)′ results, it seems probable that their results are at least moderately affected by basis set superposition error, which would artificially increase the attraction between the reacting moieties and probably lower the activation barrier. The real activation barrier might thus be larger, and the lifetime of the sCI (which depends exponentially on the barrier height) substantially longer. However, due to the complicated electronic structure and possible multireference nature of the reacting system, the B3LYP values are not quantitatively accurate enough for reliable rate predictions. As the barrier to SOZ formation is probably neither extremely large nor extremely small, very-high-level quantum chemical calculations (including both multireference effects and dynamic electron correlation) would be required to accurately determine whether or not SOZ formation is the dominating sink reaction.

Both the $(CH_3)_2COO + H_2SO_4$ and $(CH_3)_2COO + H_2O$ reactions were found to proceed with the same general mechanism, confirming that our initial guess on the nature of the sCI + H_2SO_4 reactions is correct at least for this model species. First, a hydrogen-bonded complex is formed without a barrier. Next, a proton is transferred to the COO group, followed by the formation of a new C−O bond. The transition state corresponds roughly to the midpoint of the proton-transfer process. The computations were carried out as follows. First, we optimized the hydrogen-bonded complexes and the transition states for the $(CH_3)_2COO + H_2SO_4$ and $(CH_3)_2COO + H_2O$ reactions at the B3LYP/6-311+G(2d,p)′ level. Second, we carried out a intrinsic reaction coordinate (IRC) scan[50,51] with a step size of 0.05 amu$^{1/2}$ bohr on both transition state structures. (The scans also confirmed that the transition states indeed connected the correct reactant and product structures.) To increase the reliability of the computed values (e.g., to correct for deficiencies in the DFT description of proton transfer), we then performed single-point calculations at the RI-CC2/def2-

TABLE 5: Reaction Energies and Gibbs Free Energies at 298 K for the Individual Steps of the $(CH_3)_2COO + H_2SO_4$ and $(CH_3)_2COO + H_2O$ Reactions[a]

reaction	ΔE_0, B3LYP, kcal/mol	ΔE_0, RI-CC2, kcal/mol	ΔG(298 K), B3LYP, kcal/mol
$(CH_3)_2COO + H_2SO_4 \rightleftharpoons (CH_3)_2COO\cdots H_2SO_4$	−20.48 (1.20)	−22.41[b]	−10.35
$(CH_3)_2COO\cdots H_2SO_4 \rightleftharpoons [(CH_3)_2COO\cdot H_2SO_4]^{\ddagger}$	0.088	−0.17[b,c]	−0.69
$[(CH_3)_2COO\cdot H_2SO_4]^{\ddagger} \rightleftharpoons (CH_3)_2C(OOH)-O-SO_3H$	−9.56	−16.47[b,c]	−2.92
$(CH_3)_2COO + H_2O \rightleftharpoons (CH_3)_2COO\cdots H_2O$	−9.19 (0.47)	−9.25[b]	+1.02
$(CH_3)_2COO\cdots H_2O \rightleftharpoons [(CH_3)_2COO\cdot H_2O]^{\ddagger}$	+15.22	+12.89[b,c]	+16.29
$[(CH_3)_2COO\cdot H_2O]^{\ddagger} \rightleftharpoons (CH_3)_2C(OOH)-OH$	−36.80	−37.87[b,c]	−33.76

[a] "···" denotes the hydrogen-bonded complex and "‡" denotes the transition state structure. The basis set for the B3LYP calculations was 6-311+G(2d,p) with diffuse and extra p-type polarization functions on the H_2SO_4 and H_2O hydrogen atoms. The basis set for the RI-CC2 calculations was def2-QZVPP, together with the corresponding auxiliary basis set for the RI expansion. Values in parentheses are basis set superposition errors computed using the counterpoise method. [b] Computed using the B3LYP geometry for the free molecules, hydrogen-bonded complex, and/or reaction product. [c] Maximum energy of the transition state bracketed along the B3LYP IRC path, with a step size of 0.05 amu$^{1/2}$ bohr.

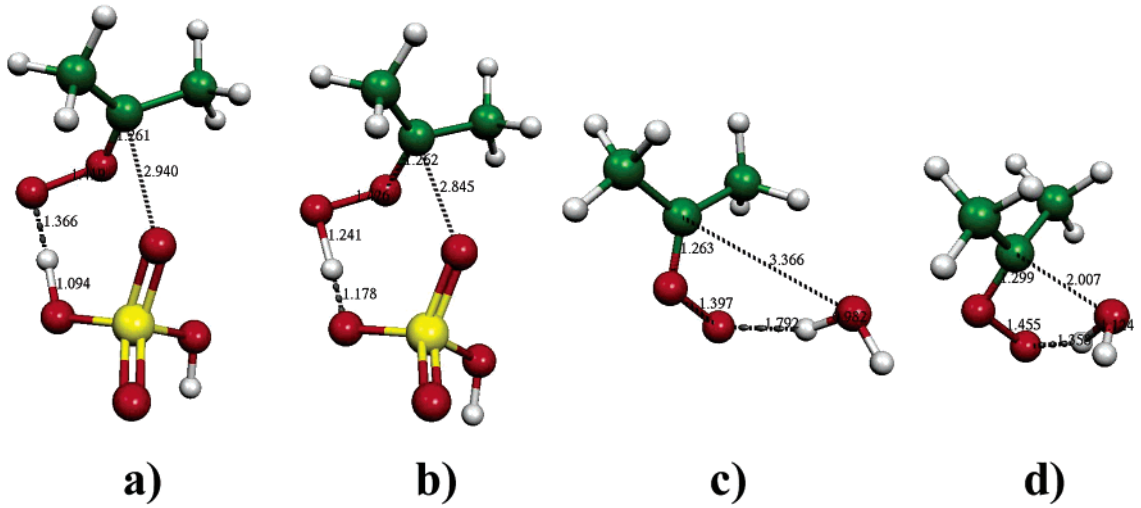

Figure 5. Structures of the hydrogen-bonded complexes and transition states formed in the reactions between $(CH_3)_2COO$ and water or sulfuric acid optimized at the B3LYP/6-311+G(2d,p) level, with diffuse basis functions and an additional set of p-type polarization functions on the H_2O and H_2SO_4 hydrogen atoms. Selected bond lengths and other interatomic distances are displayed. (a) $(CH_3)_2COO\cdots H_2SO_4$, (b) $[(CH_3)_2COO\cdot H_2SO_4]^{\ddagger}$, (c) $(CH_3)_2COO\cdots H_2O$, and (d) $[(CH_3)_2COO\cdot H_2O]^{\ddagger}$.

QZVPP level on the optimized points of the B3LYP IRC path. This allowed us to bracket the RI-CC2/def2-QZVPP maximum energy along the path, resulting in a somewhat more accurate estimate of the higher level activation energy as described by Malick et al.[52] It should be noted that the values of the D_1 diagnostic[53] computed during the RI-CC2 calculations were quite high (around 0.24 for the free sCI and 0.15 for the transition states), indicating a significant multireference nature. All values for the D_1 diagnostics are given in the Supporting Information. Thus, while the RI-CC2 activation barriers are probably more accurate than the B3LYP ones, they still cannot be considered to be quantitatively reliable. However, based on the comparisons of B3LYP and coupled-cluster methods with multireference calculations of Cremer et al.[27] and Pérez-Casany et al.,[47] the results presented here are probably qualitatively trustworthy.

The results of the activation barrier calculations (including basis set superposition errors computed using the counterpoise method[54]) are presented in Table 5, and the structures of the hydrogen-bonded complexes and transition states are displayed in Figure 5. The imaginary frequencies and reduced masses corresponding to the reaction mode coordinate, and the zero-dimensional tunneling factors calculated from the imaginary frequency using the Wigner expression,[55,56] are given in Table 6. It can be seen from Table 5 that the activation barrier of the $(CH_3)_2COO + H_2SO_4$ reaction is significantly lower than that of the $(CH_3)_2COO + H_2O$ reaction. Indeed, the RI-CC2/def2-QZVPP single-point calculations indicate that the $(CH_3)_2COO + H_2SO_4$ reaction is barrierless. It should be noted that

TABLE 6: Imaginary Frequencies ν (in wavenumbers), Corresponding Reduced Masses μ (in atomic units), and Zero-Dimensional Wigner Tunneling Factors κ, Computed from the Transition States of the $(CH_3)_2COO + H_2SO_4$ and $(CH_3)_2COO + H_2O$ Reactions at the B3LYP/6-311+G(2d,p) Level, with Diffuse and Extra p-Type Polarization Functions on the H_2SO_4 and H_2O Hydrogen Atoms

reaction	ν, cm^{-1}	μ, au	k
$(CH_3)_2COO + H_2SO_4$	289.194i	1.7266	1.08
$(CH_3)_2COO + H_2O$	754.536i	1.8996	1.55

Aplincourt and Ruiz-Lopez[26] made the same prediction for the somewhat analogous $H_2COO + SO_2$ reaction. Also, it can be seen that the RI-CC2/def2-QZVPP method predicts a somewhat more negative overall reaction energy for the $(CH_3)_2COO + H_2O$ and $(CH_3)_2COO + H_2SO_4$ reactions than the B3LYP/6-311+G(2d,p)′ method, with the difference being ca. −10 kcal/mol for the reaction with sulfuric acid and ca. −4 kcal/mol for the reaction with water. Similar differences were found between B3LYP and CCSD(T) results reported by Anglada et al.[36] However, the activation barriers (with respect to the hydrogen-bonded complexes) predicted by the two methods differ by less than 0.3 kcal/mol for the reaction with sulfuric acid and less than 3 kcal/mol for the reaction with water.

The energy parameters calculated for the $(CH_3)_2COO + H_2O \rightleftharpoons (CH_3)_2COO\cdots H_2O$ and $(CH_3)_2COO\cdots H_2O \rightleftharpoons [(CH_3)_2COO\cdot H_2O]^{\ddagger}$ reaction steps agree reasonably well with those computed by Anglada et al.,[36] who reported ΔG values of −0.4 and +15.8 kcal/mol for the first and second steps, respectively, using a combination of CCSD(T)/6-311+G(2d,2p) energies, B3LYP/

6-311+G(2d,2p), geometries and B3LYP/6-31G(d,p) vibrational frequencies. (Here "···" denotes the hydrogen-bonded complex and "‡" denotes the transition state structure.) They also reported that the basis set superposition error (BSSE) for the hydrogen-bonded complex at this level is around 1.1 kcal/mol. Our smaller value of 0.47 kcal/mol is probably mostly due to the diffuse functions added to the water hydrogen atoms. Given the error sources inherent in the computational methods themselves (e.g., due to the multireference nature of the sCI), it is clear that BSSE is a relatively insignificant error source for the 6-311+G(2d,p)′ basis set used in our activation barrier calculations. It should, however, be noted that the electronic energy component of the activation barrier calculated by Anglada et al. at the B3LYP level using the small 6-31G(d,p) basis was 4.8 kcal/mol lower than that calculated at the B3LYP/6-311+G(2d,2p) level. This supports our earlier argument that the SOZ formation barriers reported by Chuong et al.,[17] using the even smaller 6-31G(d) basis, may be significantly affected by basis set superposition.

The structure of the $(CH_3)_2COO\cdots H_2SO_4$ complex shown in Figure 5 shows some surprising features. The O−O bond length has increased from 1.380 Å (corresponding to the free sCI) to 1.419 Å, while the hydrogen bond length between the SOH and COO moieties is only 1.366 Å. (Corresponding values for the $(CH_3)_2COO\cdots H_2O$ complex are 1.397 and 1.797 Å, respectively.) This is probably related to the fact that the $(CH_3)_2COO\cdots H_2SO_4$ complex is very close to the $[(CH_3)_2COO\cdot H_2SO_4]^‡$ transition state in terms of both the molecular geometry and the energy. The very short hydrogen bond length is related to the strong attraction between the SOH and COO groups, which is demonstrated by the large binding energy of over 20 kcal/mol. Thus, the proton is probably already to some degree shared between the groups, instead of being "bonded" to just the S−O oxygen and only "H-bonded" to the COO oxygen. It is also possible that the $(CH_3)_2COO\cdots H_2SO_4$ minimum geometry is an artifact of the B3LYP method, and that the true $(CH_3)_2COO + H_2SO_4$ reaction proceeds directly to the $(CH_3)_2C(OOH)-O-SO_3H$ product. This is partially supported by the observation that the RI-CC2/def2-QZVPP single-point calculations predict the transition state to be lower in energy than the H-bonded complex. To test this hypothesis, we optimized the $(CH_3)_2COO\cdots H_2SO_4$ structure at the RI-CC2/def2-TZVPP level starting from the B3LYP geometry. This had very little effect on the CO−O bond length (which increased by 0.002 Å to 1.421 Å), while the hydrogen bond length was even further shortened to 1.309 Å. However, a subsequent numerical frequency calculation (using a step size of 0.01 au and an SCF convergence criterion of 10^{-8} au) indicated that the structure was a transition state, with an imaginary vibrational mode of 94i cm^{-1}. We were unable to find a hydrogen-bonded minimum structure at the RI-CC2 level. These findings indicate that the H-bonded complex found at the B3LYP level may well be an artifact, and that the real reaction could be totally barrierless. It should be noted that our central conclusions are insensitive to whether or not the $(CH_3)_2COO + H_2SO_4$ reaction is completely barrierless or has a very small barrier with a corresponding highly distorted shallow H-bonded minimum geometry.

The activation barriers computed here confirm our hypothesis that the reactions of sCIs with sulfuric acid are several orders of magnitude faster than those with water. Indeed, a naive application of conventional transition state theory (which states that reaction rates depend exponentially on the Gibbs free energies of activation) would imply that the $(CH_3)_2COO + H_2SO_4$ reaction, with an activation free energy very close to zero, should proceed about $10^{10}-10^{11}$ times faster than the $(CH_3)_2COO + H_2O$ reaction, for which the computed activation free energies are around 13−16 kcal/mol (depending on whether the B3LYP of RI-CC2 electronic energies are used, and whether the reaction is assumed to proceed via the H-bonded complex or directly from the reactants). However, we emphasize that the quantum chemical parameters presented here are not accurate enough for actual quantitative rate constant predictions, and that tunneling processes not represented by the zero-dimensional Wigner coefficient may increase the rate of the sCI + water reactions significantly. In terms of the experimental relative rate constants given in Table 1, we can nevertheless conclude that the relative rate constants for $sCI + H_2SO_4$ reactions are likely to be at least as large as those determined for organic acids, and might be significantly larger. This would imply that a significant fraction of the sCIs formed in atmospheric conditions may react with sulfuric acid. However, it remains to be conclusively determined whether or not the bimolecular reaction with free water molecules is the main sink reaction for the biogenic sCIs. Competing sink reactions include the unimolecular SOZ formation, and also the reactions with water clusters,[57] which are likely to have significantly lower activation barriers than those with water monomers. (It should be noted that the effect of the water clusters on the reaction rate is already implicitly included in the experimental relative rates, though not the computational ones.) These alternative sink reactions could conceivably lower the lifetime of biogenic sCIs to the point where the yield of $sCI + H_2SO_4$ reaction products is too low to have any atmospheric significance.

Conclusions

We have studied the reactions of five stabilized Criegee intermediates—three small model species and two large biogenic molecules—with sulfuric acid using quantum chemical methods, and we compared the obtained data to two competing sink reactions. All reactions were found to be at least moderately exothermic at 298 K. Intrinsic reaction coordinate calculations with high-level single-point energy evaluations indicate that the reaction of sCIs with sulfuric acid should proceed significantly faster than the reaction with water. Our results show that if a significant fraction of biogenic sCIs live long enough to undergo bimolecular reactions, then the reaction between sCIs and sulfuric acid may play an important role in the atmosphere. If, on the other hand, SOZ formation is found to be the dominating sink reaction, then investigation of an SOZ−sulfuric acid reaction might be warranted. This will be explored in a future study.

Acknowledgment. We would like to thank the Academy of Finland (Grants 211483 and 211484) for funding and the CSC (Center for Scientific Computing) for the computer time. We would also like to thank Johanna Blomqvist at CSC for her advice.

Supporting Information Available: Cartesian coordinates of all presented structures, along with the energies, enthalpies, and entropies. This material is available free of charge via the Internet at http://pubs.acs.org.

References and Notes

(1) Boucher, O.; Haigh, J.; Hauglustaine, D.; Haywood, J.; Myhre, G.; Nakajima, T.; Shi, G. Y.; Solomon, S. *Climate change 2001: The scientific basis*; IPCC; Cambridge University Press: Cambridge, U.K., 2001.

(2) Stieb, D. M.; Judek, S.; Burnett, R. T. *J. Air Manage. Assoc.* **2002**, *52*, 470.

(3) Korhonen, P.; Kulmala, M.; Laaksonen, A.; Viisanen, Y.; McGraw, R.; Seinfeld, J. H. *J. Geophys. Res.* **1999**, *104*, 26349.
(4) Anttila, T.; Vehkamäki, H.; Napari, I.; Kulmala, M. *Boreal Environ. Res.* **2005**, *10*, 511.
(5) Kulmala, M.; Vehkamäki, H.; Petäjä, T.; Dal Maso, M.; Lauri, A.; Kerminen, V.-M.; Birmili, W.; McMurry, P. H. *J. Aerosol. Sci.* **2004**, *35*, 143.
(6) Kulmala, M.; Lehtinen, K. E. J.; Laaksonen, A. *Atmos. Chem. Phys.* **2006**, *6*, 787.
(7) Weber, R. J.; Marti, J. J.; McMurry, P. H.; Eisele, F. L.; Tanner, D. J.; Jefferson, A. *Chem. Eng. Commun.* **1996**, *151*, 53.
(8) Zhang, R.; Suh, I.; Zhao, J.; Zhang, D.; Fortner, E. C.; Tie, X.; Molina, L. T.; Molina, M. J. *Science* **2004**, *304*, 1487.
(9) Seinfeld, J. H.; Pandis, S. N. *Atmospheric Chemistry and Physics: From Air Pollution to Climate Change*; Wiley & Sons: New York, 1998.
(10) Winterhalter, R.; Neeb, P.; Grossmann, D.; Kolloff, A.; Horie, O.; Moortgat, G. K. *J. Atmos. Chem.* **2000**, *35*, 165.
(11) Kückelmann, U.; Warscheid, B.; Hoffmann, T. *Anal. Chem.* **2000**, *72*, 1905.
(12) Kamens, R.; Jang, M.; Chien, C.-J.; Leach, K. *Environ. Sci. Technol.* **1999**, *33*, 1430.
(13) Bonn, B.; Schuster, G.; Moortgat, G. K. *J. Phys. Chem. A* **2002**, *106*, 2869.
(14) Bonn, B.; Moortgat, G. K. *Geophys. Res. Lett.* **2003**, *30*, 1585. DOI: 10.1029/2003GL017000.
(15) Bonn, B. Ph.D. Thesis, University of Mainz, Mainz, 2002.
(16) Criegee, R. *Angew. Chem.* **1975**, *87*, 765.
(17) Chuong, B.; Zhang, J. Y.; Donahue, N. M. *J. Am. Chem. Soc.* **2004**, *126*, 12363.
(18) Tolocka, M. P.; Heaton, K. J.; Dreyfus, M. A.; Wang, S.; Zordan, C. A.; Saul, T. D.; Johnston, M. V. *Environ. Sci. Technol.* **2006**, *40*, 1843.
(19) Bonn, B.; Korhonen, H.; Petäjä, T.; Boy, M.; Kulmala, M. *Atmos. Chem. Phys. Discuss.* **2007**, *7*, 3901.
(20) Bonn, B.; Kulmala, M.; Riipinen, I.; Sihto, S.-L.; Ruuskanen, T. M. Submitted for publication in *J. Aerosol. Sci.* **2007**.
(21) Su, F.; Calvert, J. G.; Shaw, J. H. *J. Phys. Chem.* **1980**, *84*, 239.
(22) Hatakeyama, S.; Kobayashi, H.; Akimoto, H. *J. Phys. Chem.* **1984**, *88*, 4736.
(23) Neeb, P.; Horie, O.; Moortgat, G. K. *J. Phys. Chem. A* **1998**, *102*, 6778.
(24) Neeb, P.; Sauer, F.; Horie, O.; Moortgat, G. K. *Atmos. Environ.* **1997**, *31*, 1417.
(25) Tobias, H. J.; Ziemann, P. J. *J. Phys. Chem. A* **2001**, *105*, 6129.
(26) Aplincourt, P.; Ruiz-López, M. F. *J. Am. Chem. Soc.* **2000**, *122*, 8990.
(27) Cremer, D.; Kraka, E.; Szalay, P. G. *Chem. Phys. Lett.* **1998**, *292*, 97.
(28) Zhang, D.; Lei, W.; Zhang, R. *Chem. Phys. Lett.* **2002**, *358*, 171.
(29) Chen, B.-Z.; Anglada, J. M.; Huang, M.-B.; Kong, F. *J. Phys. Chem. A* **2002**, *106*, 1877.
(30) Zhang, D.; Zhang, R. *J. Am. Chem. Soc.* **2002**, *124*, 2692.
(31) Kroll, J. H.; Sahay, S. R.; Anderson, J. G.; Demerjian, K. L.; Donahue, N. M. *J. Phys. Chem. A* **2001**, *105*, 4446.
(32) Fenske, J. D.; Kuwata, K. T.; Houk, K. N.; Paulson, S. E. *J. Phys. Chem. A* **2000**, *104*, 7246.
(33) Gutbrod, R.; Kraka, E.; Schindler, R. N.; Cremer, D. *J. Am. Chem. Soc.* **1997**, *119*, 7330.
(34) Anglada, J. M.; Bofill, J. M.; Olivella, S.; Solé, A. *J. Am. Chem. Soc.* **1996**, *118*, 4636.
(35) Crehuet, R.; Anglada, J. M.; Bofill, J. M. *Chem.—Eur. J.* **2001**, *7*, 2227.
(36) Anglada, J. M.; Aplincort, P.; Bofill, J. M.; Cremer, D. *Chem. Phys. Chem.* **2002**, *2*, 215.
(37) Mansergas, A.; Anglada, J. M. *J. Phys. Chem. A* **2006**, *110*, 4001.
(38) Frisch, M. J.; Trucks, G. W.; Schlegel, H. B.; Scuseria, G. E.; Robb, M. A.; Cheeseman, J. R.; Montgomery, J. A., Jr.; Vreven, T.; Kudin, K. N.; Burant, J. C.; Millam, J. M.; Iyengar, S. S.; Tomasi, J.; Barone, V.; Mennucci, B.; Cossi, M.; Scalmani, G.; Rega, N.; Petersson, G. A.; Nakatsuji, H.; Hada, M.; Ehara, M.; Toyota, K.; Fukuda, R.; Hasegawa, J.; Ishida, M.; Nakajima, T.; Honda, Y.; Kitao, O.; Nakai, H.; Klene, M.; Li, X.; Knox, J. E.; Hratchian, H. P.; Cross, J. B.; Bakken, V.; Adamo, C.; Jaramillo, J.; Gomperts, R.; Stratmann, R. E.; Yazyev, O.; Austin, A. J.; Cammi, R.; Pomelli, C.; Ochterski, J. W.; Ayala, P. Y.; Morokuma, K.; Voth, G. A.; Salvador, P.; Dannenberg, J. J.; Zakrzewski, V. G.; Dapprich, S.; Daniels, A. D.; Strain, M. C.; Farkas, O.; Malick, D. K.; Rabuck, A. D.; Raghavachari, K.; Foresman, J. B.; Ortiz, J. V.; Cui, Q.; Baboul, A. G.; Clifford, S.; Cioslowski, J.; Stefanov, B. B.; Liu, G.; Liashenko, A.; Piskorz, P.; Komaromi, I.; Martin, R. L.; Fox, D. J.; Keith, T.; Al-Laham, M. A.; Peng, C. Y.; Nanayakkara, A.; Challacombe, M.; Gill, P. M. W.; Johnson, B.; Chen, W.; Wong, M. W.; Gonzalez, C.; Pople, J. A. Gaussian 03, revision C.02; Gaussian, Inc.: Wallingford, CT, 2004.
(39) Ahlrichs, R.; Bär, M.; Häser, M.; Horn, H.; Kölmel, C. *Chem. Phys. Lett.* **1989**, *162*, 165.
(40) Häser, M.; Ahlrichs, R. *J. Comput. Chem.* **1989**, *10*, 104.
(41) Becke, A. D. *J. Chem. Phys.* **1993**, *98*, 5648.
(42) Lee, C.; Yang, W.; Parr, R. G. *Phys. Rev. B* **1988**, *37*, 785.
(43) Christiansen, O.; Koch, H.; Jørgensen, P. *Chem. Phys. Lett.* **1995**, *243*, 409.
(44) Hättig, C.; Weigend, F. *J. Chem. Phys.* **2000**, *113*, 5154.
(45) Weigend, F.; Ahlrichs, R. *Phys. Chem. Chem. Phys.* **2005**, *18*, 3297.
(46) Hättig, C. *Phys. Chem. Chem. Phys.* **2005**, *7*, 59.
(47) Pérez-Casany, M. P.; Nebot-Gil, I.; Sánchez-Marín, J. *J. Phys. Chem. A* **2000**, *104*, 6277.
(48) Sakai, S. *Internet Electron. J. Mol. Des.* **2002**, *1*, 462.
(49) Portmann, S.; Fluekiger, P. F. *MOLEKEL*, version 4.3.win32; CSCS/University of Geneva: Geneva, Switzerland, 2002.
(50) Gonzales, C.; Schlegel, H. B. *J. Chem. Phys.* **1989**, *90*, 2154.
(51) Gonzales, C.; Schlegel, H. B. *J. Phys. Chem.* **1990**, *94*, 5523.
(52) Malick, D. K.; Petersson, G. A.; Montgomery, J. A., Jr. *J. Chem. Phys.* **1998**, *108*, 5704.
(53) Janssen, C. L.; Nielsen, I. M. B. *Chem. Phys. Lett.* **1998**, *290*, 423.
(54) Boys, S. F.; Bernadfi, F. *Mol. Phys.* **1970**, *19*, 553.
(55) Wigner, E. P. *Z. Phys. Chem., Abt. B* **1932**, *19*, 203.
(56) Rapp, D. *Statistical Mechanics*; Holt, Rinehart & Winston: New York, 1972.
(57) Ryzhkov, A. B.; Ariya, P. A. *Chem. Phys. Lett.* **2006**, *419*, 497.